American Mineralogist, Volume 82, pages 760–764, 1997

Ab-initio synthesis and TEM confirmation of antigorite in the system MgO-SiO_2-H_2O

BERND WUNDER,[1] ALAIN BARONNET,[2]* AND WERNER SCHREYER[1]

[1]Research Group on High-Pressure Metamorphism, Institut für Mineralogie, Ruhr-Universität Bochum, D-44780 Bochum, Germany

[2]Centre de Recherche sur les Mécanismes de la Croissance Cristalline, Campus Luminy, Case 913, 13288 Marseille Cedex 9, France

ABSTRACT

For the first time, chemically pure, nearly single-phase antigorite, $Mg_{48}Si_{34}O_{85}(OH)_{62}$, was synthesized directly without using seeds. Starting material was a stoichiometric mixture of previously synthesized talc and brucite. Synthesis conditions were 50 kbar, 500 °C, and 120 h. TEM studies show that the dominant wavelength for the structural modulation of antigorite is about 4.5 nm, which corresponds to $m = 17$ in the general antigorite formula $M_{3m-1}T_{2m}O_{5m}(OH)_{4m-6}$ and thus to the structure of most natural antigorites. Selected-area electron diffraction patterns of single crystals exhibit the $hk0$ reciprocal net diagnostic of antigorite.

INTRODUCTION

Antigorite is one of the three common varieties of serpentine, namely the flat-layered lizardite, the rolled-layered chrysotile, and the modulated-layered antigorite (Wicks and O'Hanley 1988). Its structure consists mainly of positional modulations of the curved 1:1 silicate layer along the a axis. Although the structural continuity of both the tetrahedral and octahedral sheets is maintained, the modulation is due to the periodic reversal of the layer polarity (and of silicate tetrahedra) making half-waves. The modulation wavelengths may range from 3.3 to 10 nm (Zussman et al. 1957; Kunze 1961; Uehara and Shirozu 1985; Mellini and Zussman 1986; Mellini et al. 1987). The modulations are commensurate to one-half the lizardite lattice distance along a because an integral number of silicate tetrahedra form the half-wave. At locations where such reversals occur the structure may be seen as a narrow module of talc otherwise separating larger domains of ideal serpentine structure, making antigorite a modular structure also (Spinnler 1985; Ferraris et al. 1986). For these structural reasons, the chemical composition of antigorite deviates more or less from that of ideal serpentine, $Mg_3Si_2O_5(OH)_4$, toward that of talc, $Mg_3Si_4O_{10}(OH)_2$, for the shortest modulation wavelengths.

Transmission electron microscopy (TEM) studies of natural antigorite deal mostly with modulation microstructures including dislocations and twinning, polytypism, defects, and textural relationships with other members of the serpentine group (Spinnler 1985; Otten 1993; Mellini et al. 1987). Modulation contrasts are best seen when looking along [010] or along the normal to the average layer plane.

Antigorite is a very difficult phase to synthesize because of its sluggish nucleation rate. After many unsuccessful and questionable attempts reported in the literature (Jasmund and Sylla 1972; Ishi and Saito 1973), Johannes (1975) was first to synthese antigorite in appreciable amounts, but only after very long experiments (56 d) at 15 kbar and 580 °C. Starting material was an oxide mixture or a mixture of talc and forsterite seeded with 1% natural Fe,Al-containing antigorite. This material was later used by Evans et al. (1976) for their equilibrium experiments. Wunder and Schreyer (1997), using gels seeded with natural antigorite as starting materials, did not observe any clear formation of antigorite after experiment durations of up to three weeks at the same P-T conditions used by Johannes (1975).

Here we report a simple method for the synthesis of pure antigorite within the system MgO-SiO_2-H_2O (MSH) from previously synthesized talc and brucite and present TEM evidence that the product really represents antigorite.

EXPERIMENTAL METHODS

The high-pressure experiments were performed in a piston-cylinder apparatus as constructed after Boyd and England (1960). The type of pressure cells as well as the relative positions of the mantled chromel-alumel thermocouple and the gold tube (8 mm in length) containing the sample within the pressure cell are the same as depicted by Massonne and Schreyer (1986, their Fig. 2, pressure cell type II). In each experiment the gold tube was filled with about 10 mg of the crystalline starting material, plus 20 wt% distilled water.

Starting materials for the formation of pure MSH antigorite were mixtures of brucite and talc, both synthesized as pure MSH phases. Conditions of synthesis for

* Also associated with the universities of Aix-Marseille II and III.

0003–004X/97/0708–0760$05.00

TABLE 1. Results of high-pressure experiments for the synthesis of antigorite

Experiment no.	Starting composition	Crystalline products
239	brucite plus talc in the proportion Mg/Si = 48/34, 5% natural antigorite seeds	antigorite, small amounts of brucite
241/2	brucite plus talc in the proportion Mg/Si = 48/34	antigorite, small amounts of brucite
254	brucite plus talc in the proportion Mg/Si ≈ 48/35	antigorite, small amounts of talc, little chrysotile (from TEM study)
287	brucite plus talc in the proportion Mg/Si ≈ 96/69	antigorite, very small amounts of brucite (see Fig. 2)

Notes: In each experiment 20 wt% water was added to the crystalline starting material. Experiment conditions were P = 50 kbar, T = 500°C, t = 120 h for each experiment.

these phases as well as their cell-dimensions were given by Wunder and Schreyer (1997). Small amounts of periclase were observed by X-ray diffraction within the sample of brucite. In the first antigorite synthesis experiment (Table 1, experiment no. 239) the brucite and talc mixture was seeded with natural antigorite from the locality Piz Lunghin, Switzerland, also used by Johannes (1975). Chemical and physical characterization of this material was also given by Wunder and Schreyer (1997).

Products of experiment no. 254 (Table 1) were treated ultrasonically in doubly distilled water before a drop of the suspension was allowed to evaporate slowly on the surface of a carbon film, which in turn was mounted on a conventional mesh copper grid. A JEOL 2000 FX electron microscope operating at 200 kV was used for imaging and electron diffraction of the layer silicates.

SYNTHESIS OF ANTIGORITE

All the possible compositional and structural varities of antigorite, which can be expressed, according to Kunze (1961), by the formula $M_{3m-1}T_{2m}O_{5m}(OH)_{4m-6}$ (m = number of tetrahedra in a single chain defined by the wavelength, M = octahedral cations, T = tetrahedral cations), lie along the join between brucite and talc in the MSH system (Fig. 1). Therefore, reactions to form antigorite from brucite and talc are necessarily degenerate and water-conserving. To test this reaction also as a possible upper pressure stability limit of antigorite, talc and brucite were first mixed in the proportions of an antigorite with composition $Mg_{48}Si_{34}O_{85}(OH)_{62}$ (m = 17) and seeded with 5 wt% of the natural antigorite. This composition was chosen because this formula is often cited in the literature (e.g., Kunze 1961; Chernosky et al. 1991) as a typical MSH composition for antigorite. However, it is also known [e.g., from the work of Mellini et al. (1987) who studied the compositions and structural states of natural antigorites] that m values may vary between 23 and 14. Although no H_2O is consumed or released during the theoretical reaction mentioned above, water was added to increase the rate of reaction.

After 5 d at 50 kbar and 500 °C the product of the first seeded experiment (Table 1, experiment no. 239), as characterized by X-ray diffraction, consisted of only antigo-

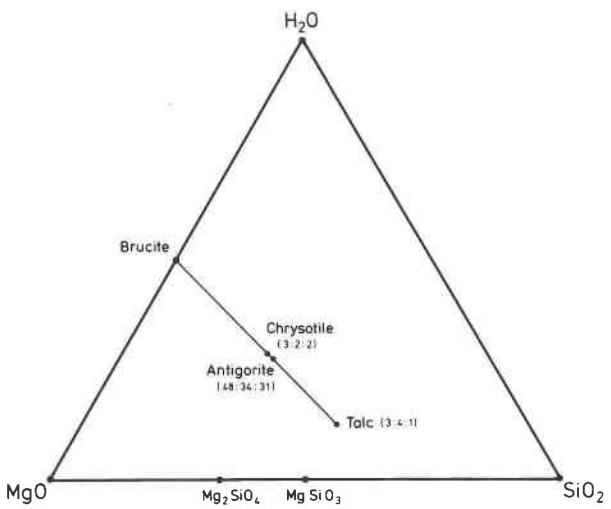

FIGURE 1. Selected phases in the system MgO-SiO_2-H_2O (MSH). The molar ratios of MgO:SiO_2:H_2O are given in parentheses. Solid line emphasizes the colinearity of compositions of brucite, chrysotile, antigorite, and talc.

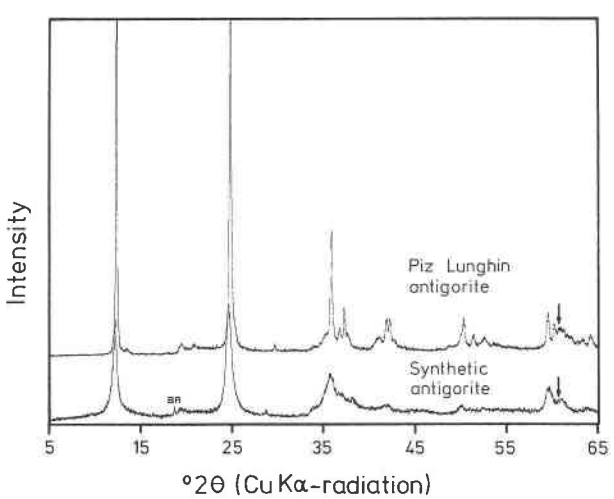

FIGURE 2. X-ray powder diffraction pattern of the synthesis product of experiment no. 287 (Table 1) in comparison with that for natural antigorite from Piz Lunghin, Switzerland. BR marks the faint 001 reflection of brucite, and arrows indicate the critical antigorite reflection after Peacock (1987). For further explanations see text.

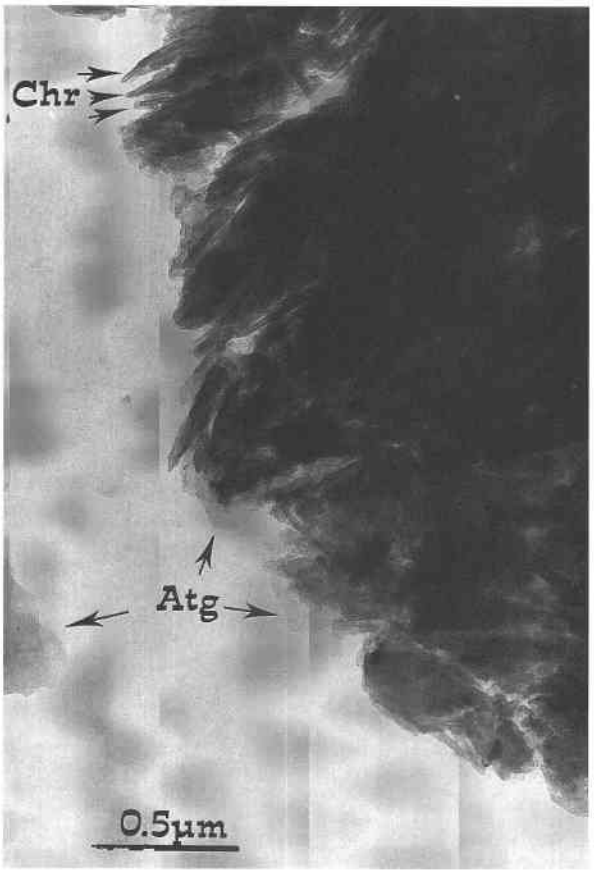

FIGURE 3. Low-magnification TEM image of the products of experiment 254. Chr = chrysotile rolls with hollow cores; Atg = antigorite crystals.

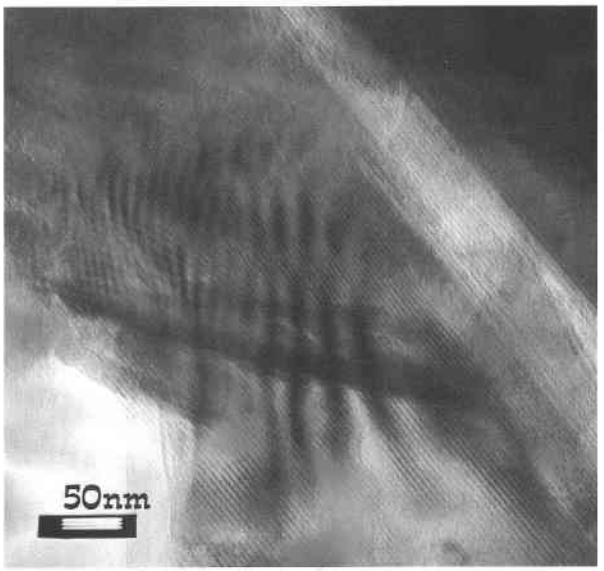

FIGURE 4. TEM image of a part of an antigorite flake viewed normal to the layers. Narrowest, straight stripes, 4.5 nm apart, mark the modulation contrast, whereas the widest, curved stripes are Moiré patterns.

rite and small amounts of brucite; talc was totally consumed. The characteristic antigorite reflection at d = 1.53 Å, distinguishing antigorite from the other serpentine phases chrysotile and lizardite (Peacock 1987), was rather faint (cf. Fig. 2). A second experiment (Table 1, experiment no. 241/2) at the same P-T and time conditions, and starting with the same brucite and talc mixture and the same water content, but without any natural antigorite seeds, led to an identical result. Thus, for the first time, it seemed that an ab-initio method for the synthesis of pure MSH antigorite has been found.

The small amounts of brucite obtained during the two antigorite synthesis experiments 239 and 241/2 (Table 1) may perhaps be explained as follows. In TEM studies of the talc used here for antigorite synthesis small amounts of 5 Å layers were observed, which are probably brucite-like sheets (Wunder et al. 1996). Occurrence of such chlorite-like configurations within talc might be due to a compositional shift of the starting material as a result of SiO_2 leaching during talc synthesis. Together with the small amounts of periclase observed during brucite synthesis, this might lead to a higher MgO content for the starting mixture than the desired $Mg_{48}Si_{34}O_{85}(OH)_{62}$ composition of antigorite. This Mg enrichment in the solids might be increased due to a still higher solubility of SiO_2 during antigorite synthesis because, after Manning (1994), SiO_2 solubility in the pure SiO_2-H_2O system is about 1–2 wt% at the P-T conditions of 50 kbar and 500 °C.

A third experiment (254, Table 1) at the same P-T and time conditions, but with a slightly higher amount of talc compared to the two earlier experiments, resulted in antigorite plus small amounts of talc, as determined by X-ray diffraction. No significant shift in the 2θ positions of the very broad antigorite reflections observed in this experiment was detected when compared to those from the other experiments (Table 1). The material synthesized in experiment no. 254 was used for the TEM study to determine the structural state of the MSH antigorite as well as its chemistry.

After the TEM study on experiment no. 254 a fourth synthesis experiment (287, Table 1) was performed at the same P-T and time condititions, but with a mixture of brucite plus talc in the proportion Mg/Si ≈ 96/69. This experiment resulted in still higher yields of nearly single-phase antigorite. The very faint reflection at 2θ = 18.6° (Fig. 2) might be due to the strong 001 reflection of brucite.

The X-ray powder diffraction reflections of the synthetic MSH antigorite are much broader than those of the natural antigorite from the Piz Lunghin locality (Fig. 2). Therefore, no reliable cell dimensions could be determined for our material. The broadness of the reflections may be due to the small grain size of the antigorite crystals or perhaps to mixtures of different structural states, which is addressed by the TEM study.

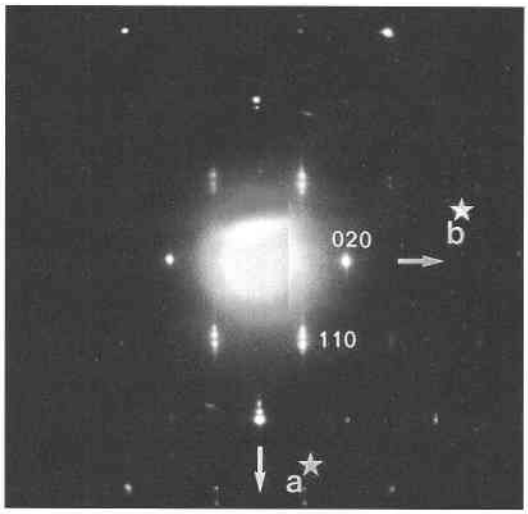

FIGURE 5. Selected-area electron diffraction pattern of a single flake of synthetic antigorite with a regular modulation wavelength; *hk*0 reciprocal net. Note that the satellite spots are more visible near 110-type reflections than near 020-type reflections.

TEM STUDY

The product of experiment 254 (Table 1) displays dominant antigorite ($\gtrsim$ 80%), minor talc, and subsidiary chrysotile (Fig. 3). Talc is recognized by bright reflections of the 020 and 110 types and by analytical electron microscopy (Mg/Si = 0.75). Chrysotile is identified by the tubular morphology of individual fibers (see also Fig. 3).

Antigorite forms anhedral to sub-euhedral flakes (Fig. 3) with highly variable widths (100–600 nm) and thicknesses (~ 4–140 nm) measured from edge-on crystals. Observed along the normal to the flakes most particles display faint black and white stripes of modulation contrast with nearly 4.5 nm periodicity and some Moiré patterns that are due to the interference of these modulations (Fig. 4). Selected-area electron diffraction (SAED) patterns of single crystals exhibiting the *hk*0 reciprocal net (Fig. 5) are diagnostic for antigorite. In the vicinity of each intense *hk*0 reflection, substructure reflections are aligned along a^* and characterize periodic lattice modulation. Intensity profile measurements and digitized SAED patterns confirm the dominant 4.5 ± 0.15 nm wavelength for the modulation, which is close to that of most natural antigorite samples. Continuous streaks may sometimes replace satellite spots: direct-space observations demonstrate that they are due either to irregular modulations in single grains or to small flake widths allowing a limited number of modulation repeats along [100]*. As-grown crystal stacks display frequent modulation twinning on (001) with $k \times 60°$ rotations of superimposed modulation patterns, which are faintly visible in direct space (Fig. 6) as well as in reciprocal space (Fig. 7).

ACKNOWLEDGMENTS

S. Nitsche and F. Quintric from CRMC2 are thanked for maintenance of the electron microscope and micrograph processing, respectively. We

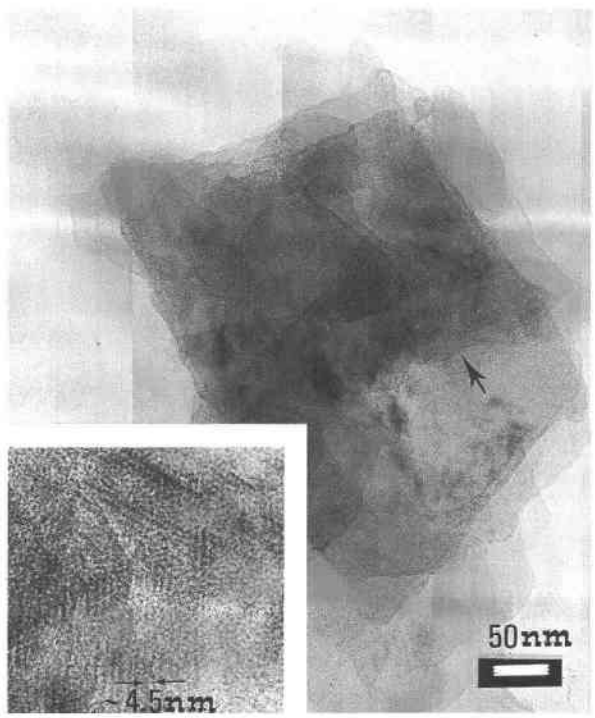

FIGURE 6. TEM image of antigorite flake showing faint modulation contrasts crosscutting each other at 60 or 120° (black arrow points to the zone numerically processed to enhance contrast as inset). This indicates modulation twinning on the antigorite basal plane.

FIGURE 7. Six star-like arrangements of satellite reflections on the antigorite 020- and 110-type subcell reflections. This is diagnostic of $k \times 60°$ rotation of twin individuals. Twin individuals are superimposed along c^* owing to modulation fringes crosscutting each other as visible in Figure 6.

thank D. Jenkins and M. Otten for their helpful reviews. Thanks are due to Deutsche Forschungsgemeinschaft for supporting the work under the auspices of the Research Group.

References cited

Boyd, F.R. and England, J.L. (1960) Apparatus for phase-equilibrium measurements at pressures up to 50 kbars and temperatures up to 1750 °C. Journal of Geophysical Research, 65, 741–748.

Chernosky, J.V., Berman, R.G., and Bryzndzia, L.T. (1991) Stability, phase relations, and thermodynamic properties of chlorite and serpentine group minerals. In Mineralogical Society of America Reviews in Mineralogy, 19, 295–346.

Evans, B.W., Johannes, W., Oterdoom, H., and Trommsdorff, V. (1976) Stability of chrysotile and antigorite in the serpentinite multisystem. Schweizerische Mineralogische und Petrographische Mitteilungen, 56, 79–93.

Ferraris, G., Mellini, M., and Merlino, S. (1986) Polysomatism and the classification of minerals. Rendiconti della Societa Italiana di Mineralogica e Petrologica, 41, 181–192.

Iishi, K. and Saito, M. (1973) Synthesis of antigorite. American Mineralogist, 58, 915–919.

Jasmund, K. and Sylla, H.M. (1972) Synthesis of Mg- and Ni-antigorite: a correction. Contributions to Mineralogy and Petrology, 34, 346.

Johannes, W. (1975) Zur Synthese und thermischen Stabilität von Antigorit. Fortschritte der Mineralogie, Beihefte, 53, 36.

Kunze, G. (1961) Antigorit. Strukturtheoretische Grundlagen und ihre praktische Bedeutung für die weitere Serpentin-Forschung. Fortschritte der Mineralogie, 39, 206–324.

Manning, C.E. (1994) The solubility of quartz in H_2O in the lower crust and upper mantle. Geochimica et Cosmochimica Acta, 58, 4831–4839.

Massonne, H.-J. and Schreyer, W. (1986) High-pressure synthesis and X-ray properties of white micas in the system K_2O-MgO-Al_2O_3-SiO_2-H_2O. Neues Jahrbuch für Mineralogie Abhandlungen, 153, 177–215.

Mellini, M. and Zussman, J. (1986) Carlosturanite (not picrolite) from Taberg, Sweden. Mineralogical Magazine, 50, 675–679.

Mellini, M., Trommsdorff, V., and Compagnoni, R. (1987) Antigorite polysomatism: behaviour during progressive metamorphism. Contributions to Mineralogy and Petrology, 97, 147–155.

Otten, M.T. (1993) High-resolution transmission electron microscoy of polysomatism and stacking defects in antigorite. American Mineralogist, 78, 75–84.

Peacock, S.M. (1987) Serpentinization and infiltration metasomatism in the Trinity peridotite, Klamath province, northern California: implications for subduction zones. Contributions to Mineralogy and Petrology, 95, 55–70.

Spinnler, G.E. (1985) HRTEM study of antigorite, pyroxene-serpentine reactions and chlorite. Ph.D. thesis, Arizona State University, Tempe.

Uehara, S. and Shirozu, H. (1985) Variations in chemical composition and structural properties of antigorite. Mineralogical Journal of Japan, 12, 299–318.

Wicks, F.J. and O'Hanley, D.S. (1988) Serpentine minerals: structure and petrology. In Mineralogical Society of America Reviews in Mineralogy, 19, 91–167.

Wunder, B. and Schreyer, W. (1997) Antigorite: High-pressure stability in the system MgO-SiO_2-H_2O (MSH). Lithos, (in press).

Wunder, B., Wirth, R., and Schreyer, W. (1996) Brucite-like sheets within synthetic talc: Do they influence the determination of talc-stability? Terra Nova, Abstract supplement No. 1, 8, 68.

Zussman, J., Brindley, G.W. and Comer, J.J. (1957) Electron diffraction studies of serpentine minerals. American Mineralogist, 42, 133–153.

Manuscript received August 23, 1996
Manuscript accepted February 27, 1997